

Higgs mode mediated enhancement of interlayer transport in high- T_c cuprate superconductors

Guido Homann ¹, Jayson G. Cosme ^{1,2,3}, Junichi Okamoto ^{4,5} and Ludwig Mathey^{1,2}

¹Zentrum für Optische Quantentechnologien and Institut für Laserphysik, Universität Hamburg, 22761 Hamburg, Germany

²The Hamburg Centre for Ultrafast Imaging, Luruper Chaussee 149, 22761 Hamburg, Germany

³National Institute of Physics, University of the Philippines, Diliman, Quezon City 1101, Philippines

⁴Institute of Physics, University of Freiburg, Hermann-Herder-Strasse 3, 79104 Freiburg, Germany

⁵EUCOR Centre for Quantum Science and Quantum Computing, University of Freiburg, Hermann-Herder-Strasse 3, 79104 Freiburg, Germany



(Received 26 November 2020; revised 5 March 2021; accepted 25 May 2021; published 2 June 2021)

We put forth a mechanism for enhancing the interlayer transport in cuprate superconductors, by optically driving plasmonic excitations along the c axis with a frequency that is blue-detuned from the Higgs frequency. The plasmonic excitations induce a collective oscillation of the Higgs field which induces a parametric enhancement of the superconducting response, as we demonstrate with a minimal analytical model. Furthermore, we perform simulations of a particle-hole symmetric $U(1)$ lattice gauge theory and find good agreement with our analytical prediction. We map out the renormalization of the interlayer coupling as a function of the parameters of the optical field and demonstrate that the Higgs mode mediated enhancement can be larger than 50%.

DOI: [10.1103/PhysRevB.103.224503](https://doi.org/10.1103/PhysRevB.103.224503)

I. INTRODUCTION

The observation of light-induced superconductivity in cuprates and organic salts has been associated with exciting lattice or molecular vibrations [1–3]. Related experiments on light-enhanced interlayer transport in the bilayer cuprate $\text{YBa}_2\text{Cu}_3\text{O}_{7-\delta}$ (YBCO) above and below the critical temperature T_c have been reported in Refs. [4–7]. Several mechanisms for these observations have been proposed in Refs. [8–14]. These proposed mechanisms focus on inducing phononic motion and its influence on the superconducting response. Here, we propose to enhance the interlayer transport in cuprates by optically exciting Higgs oscillations. This collective motion of the Higgs field couples parametrically to the plasma field, which results in the enhancement of the superconducting response. Our primary example will be monolayer cuprates. We expect that similar results emerge for other lattice geometries as well. We demonstrate that the enhancement of the superconducting response, in particular the low-frequency behavior of the imaginary conductivity, is achieved via driving of the electric field along the c axis with frequencies that are slightly blue-detuned from the Higgs frequency. Thus, we expand the scope of dynamical control of the superconducting state in the cuprates by exploiting nonlinear plasmonics [15,16].

In this paper, we first consider a two-mode model with a cubic coupling of the Higgs and plasma modes [17]. Based on this minimal model, we provide an analytical expression for the Higgs mode mediated renormalization of the interlayer coupling in monolayer cuprates. We then extend our treatment to a $U(1)$ lattice gauge theory with inherent particle-hole symmetry and simulate the c -axis optical conductivity for different ratios of the Higgs and plasma frequencies at zero temperature. The numerical results confirm our analytical prediction,

and we identify the optimal parameter regime for observing the Higgs mode mediated enhancement of interlayer transport. Finally, we discuss the feasibility of the effect and possible challenges brought by damping.

II. ANALYTICAL PREDICTION

Expanding on previous works [18–21], we model a layered superconductor as a stack of intrinsic Josephson junctions. In addition to Josephson plasma resonances [22–24], recent experiments have revealed the existence of another fundamental excitation in cuprate superconductors, the Higgs mode [25–27]. This mode corresponds to amplitude oscillations of the superconducting order parameter ψ , which decouples from the plasma mode in a system with approximate particle-hole symmetry [28,29]. The two distinct low-energy modes of a monolayer cuprate superconductor are depicted in Fig. 1(a), where the phase of ψ shall be interpreted as the gauge-invariant phase difference between adjacent layers. At zero momentum, the lowest-order coupling between the Higgs field h and the unitless vector potential a is given by the cubic interaction Lagrangian $\mathcal{L}_{\text{int}} \sim a^2 h$ [27,30]. The equations of motion corresponding to such a minimal model for describing the dynamics of a light-driven monolayer cuprate at zero temperature are

$$\ddot{a} + \gamma_J \dot{a} + \omega_J^2 a + 2\omega_J^2 a h = j, \quad (1)$$

$$\ddot{h} + \gamma_H \dot{h} + \omega_H^2 h + \alpha \omega_J^2 a^2 = 0, \quad (2)$$

where ω_H is the Higgs frequency, ω_J is the plasma frequency, and γ_H and γ_J are damping coefficients. The capacitive coupling constant α is of the order of 1 in the cuprates [31]. The interlayer current j is induced by an external electric field.

We use $\gamma_H/2\pi = \gamma_J/2\pi = 0.5$ THz and $\alpha = 1$ unless stated otherwise [32], and we assume the z axis to be aligned with the c axis of the crystal.

For weak pump-probe strengths, we perform a perturbative expansion for a and h around their equilibrium values [32]. To calculate the c -axis optical conductivity $\sigma(\omega)$ in the driven state, we apply both driving and probing currents. We take the current as a first-order term in the expansion, i.e.,

$$j = \lambda(j_{\text{dr},1}e^{-i\omega_{\text{dr}}t} + j_{\text{pr},1}e^{-i\omega_{\text{pr}}t} + \text{c.c.}), \quad (3)$$

where $\lambda \ll 1$ is a small expansion parameter. Hence, the leading contribution to a is of first order and the leading contribution to h is of second order. The coupling term $\sim ah$

gives a third-order correction to a . Additionally, we assume that the probing frequency ω_{pr} is much smaller than the driving frequency ω_{dr} and the eigenfrequencies ω_H and ω_J . Thus, we obtain an approximate expression for the Fourier component $a(\omega_{\text{pr}}) = \lambda a_{\text{pr},1} + \lambda^3 a_{\text{pr},3}$. The contributions are $a_{\text{pr},1} \approx j_{\text{pr},1}/\omega_J^2$ and

$$a_{\text{pr},3} \approx \frac{4\alpha |j_{\text{dr},1}|^2 j_{\text{pr},1} (\omega_{\text{dr}}^2 - 3\omega_H^2 + i\gamma_H \omega_{\text{dr}})}{\omega_H^2 (\omega_{\text{dr}}^2 - \omega_H^2 + i\gamma_H \omega_{\text{dr}}) [(\omega_{\text{dr}}^2 - \omega_J^2)^2 + \gamma_J^2 \omega_{\text{dr}}^2]}. \quad (4)$$

This leads to the analytical prediction

$$\omega_{\text{pr}} \sigma(\omega_{\text{pr}}) = \frac{i\epsilon_z \epsilon_0 j(\omega_{\text{pr}})}{a(\omega_{\text{pr}})} \approx \frac{i\epsilon_z \epsilon_0 \omega_J^2 \omega_H^2 (\omega_{\text{dr}}^2 - \omega_H^2 + i\gamma_H \omega_{\text{dr}}) [(\omega_{\text{dr}}^2 - \omega_J^2)^2 + \gamma_J^2 \omega_{\text{dr}}^2]}{\omega_H^2 (\omega_{\text{dr}}^2 - \omega_H^2 + i\gamma_H \omega_{\text{dr}}) [(\omega_{\text{dr}}^2 - \omega_J^2)^2 + \gamma_J^2 \omega_{\text{dr}}^2] + 4\alpha \omega_J^2 |j_{\text{dr}}|^2 (\omega_{\text{dr}}^2 - 3\omega_H^2 + i\gamma_H \omega_{\text{dr}})}, \quad (5)$$

where ϵ_z denotes the dielectric permittivity of the junctions, and $j_{\text{dr}} = \lambda j_{\text{dr},1}$ is the driving amplitude. We define an effective Josephson coupling [13] based on the $1/\omega$ divergence of the conductivity,

$$J_{\text{eff}} = \frac{\hbar}{2ed_z} \text{Im}[\omega_{\text{pr}} \sigma(\omega_{\text{pr}})]_{\omega_{\text{pr}} \rightarrow 0}, \quad (6)$$

with the interlayer spacing d_z . In the absence of driving, the Josephson coupling is $J_0 = \hbar \epsilon_z \epsilon_0 \omega_J^2 / (2ed_z)$ according to

Eq. (5). The analytical prediction for J_{eff}/J_0 in the presence of driving is shown in Fig. 1(c). The key result of this work is the enhancement of the effective interlayer coupling when the pump frequency is slightly blue-detuned from the Higgs frequency. This enhancement phenomenon is due to parametric amplification. Indeed, Eq. (1) takes the form of a parametric oscillator due to the two-wave mixing of drive and probe in Eq. (2), inducing amplitude oscillations at frequencies $2\omega_{\text{dr}}$, $2\omega_{\text{pr}}$, and $\omega_{\text{dr}} \pm \omega_{\text{pr}}$. The coupling of amplitude oscillations with $\omega_{\text{dr}} \pm \omega_{\text{pr}}$ to the drive amplifies the current response at the probing frequency. The numerical results in Figs. 1(c) and 1(d), further highlighting the enhancement of interlayer transport, are obtained by simulating a full lattice gauge model discussed in the following.

III. LATTICE GAUGE MODEL

We now turn to our relativistic $U(1)$ lattice gauge theory in three dimensions, which is inherently particle-hole symmetric. The layered structure of cuprate superconductors is encoded in the lattice parameters. Our approach allows us to explicitly simulate the coupled dynamics of the order parameter of the superconducting state $\psi_{\mathbf{r}}(t)$ and the electromagnetic field $\mathbf{A}_{\mathbf{r}}(t)$ at temperatures below T_c . To this end, we describe the Cooper pairs as a condensate of interacting bosons with charge $-2e$, represented by the complex field $\psi_{\mathbf{r}}(t)$. The time-independent part of our model Lagrangian has the form of the Ginzburg-Landau free energy [33], discretized on an anisotropic lattice. We model the layered structure of high- T_c cuprates using an anisotropic lattice geometry as illustrated in Fig. 1(b). The in-plane discretization length d_{xy} constitutes a short-range cutoff around the coherence length, while the interlayer spacing d_z is the distance between the CuO_2 planes in the crystal. Each component of the vector potential $A_{s,\mathbf{r}}(t)$ is located at half a lattice site from site \mathbf{r} in the s direction, where $s \in \{x, y, z\}$. According to the Peierls substitution, it describes the averaged electric field along the bond of a plaquette in Fig. 1(b).

We discretize space by mapping it on a lattice and implement the compact $U(1)$ lattice gauge theory in the time

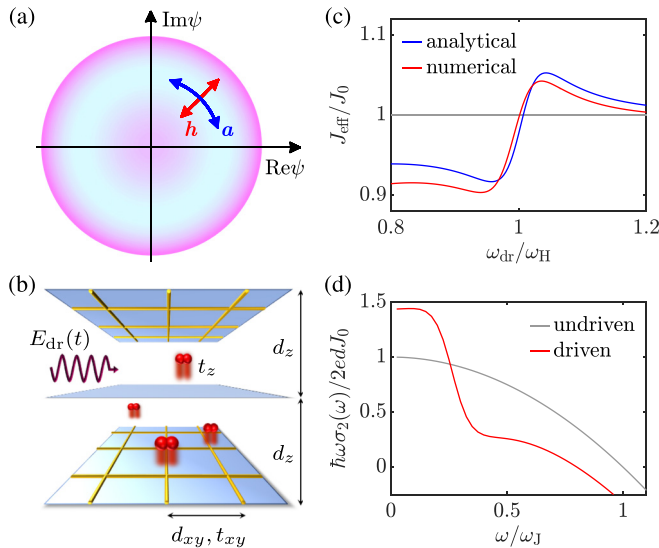


FIG. 1. (a) Higgs and plasma modes of a monolayer cuprate superconductor, illustrated with a Mexican hat potential for the superconducting order parameter. (b) Schematic representation of a layered superconductor periodically driven by a c -axis polarized electric field with frequency ω_{dr} and field strength E_0 . (c) Effective interlayer coupling J_{eff} rescaled by its equilibrium value J_0 . The field strength is fixed at $E_0 = 100$ kV/cm. (d) Numerical results for the imaginary conductivity σ_2 . The driving parameters are $\omega_{\text{dr}} = 1.05 \omega_H$ and $E_0 = 400$ kV/cm. The cuprate considered in (c) and (d) has the Josephson plasma frequency $\omega_J/2\pi = 2$ THz and the Higgs frequency $\omega_H/2\pi = 6$ THz.

continuum limit [34]. The Lagrangian of the lattice gauge model is

$$\mathcal{L} = \mathcal{L}_{\text{sc}} + \mathcal{L}_{\text{em}} + \mathcal{L}_{\text{kin}}. \quad (7)$$

The first term is the $|\psi|^4$ model of the superconducting condensate in the absence of Cooper pair tunneling,

$$\mathcal{L}_{\text{sc}} = \sum_{\mathbf{r}} K \hbar^2 |\partial_t \psi_{\mathbf{r}}|^2 + \mu |\psi_{\mathbf{r}}|^2 - \frac{g}{2} |\psi_{\mathbf{r}}|^4, \quad (8)$$

where μ is the chemical potential, and g is the interaction strength. This Lagrangian is particle-hole symmetric due to its invariance under $\psi_{\mathbf{r}} \rightarrow \psi_{\mathbf{r}}^*$. The coefficient K describes the magnitude of the dynamical term [27,29].

The electromagnetic part \mathcal{L}_{em} is the discretized form of the free-field Lagrangian:

$$\mathcal{L}_{\text{em}} = \sum_{s,\mathbf{r}} \frac{\epsilon_s \epsilon_0}{2} E_{s,\mathbf{r}}^2 - \frac{1}{\mu_0 \beta_s^2} [1 - \cos(\beta_s B_{s,\mathbf{r}})]. \quad (9)$$

Here, $E_{s,\mathbf{r}}$ denotes the s component of the electric field, and ϵ_s is the dielectric permittivity along that axis. The magnetic field components $B_{s,\mathbf{r}}$ follow from the finite-difference representation of $\nabla \times \mathbf{A}$. The temporal and spatial arrangement of the electromagnetic field is consistent with the finite-difference time-domain (FDTD) method for solving Maxwell's equations [35]. Note that we choose the temporal gauge for our calculations, i.e., $E_{s,\mathbf{r}} = -\partial_t A_{s,\mathbf{r}}$. The coefficients for the magnetic field are $\beta_x = \beta_y = 2ed_{xy}d_z/\hbar$ and $\beta_z = 2ed_{xy}^2/\hbar$.

The nonlinear coupling between the Higgs field and the electromagnetic field derives from the tunneling term

$$\mathcal{L}_{\text{kin}} = - \sum_{s,\mathbf{r}} t_s |\psi_{\mathbf{r}'(s)} - \psi_{\mathbf{r}} e^{ia_{s,\mathbf{r}}}|^2, \quad (10)$$

where $\mathbf{r}'(s)$ denotes the neighboring lattice site of \mathbf{r} in the positive s direction. The unitless vector potential $a_{s,\mathbf{r}} = -2ed_s A_{s,\mathbf{r}}/\hbar$ couples to the phase of the superconducting field, ensuring the local gauge invariance of \mathcal{L}_{kin} . The in-plane tunneling coefficient is t_{xy} , and the interlayer tunneling coefficient is t_z .

We numerically solve the equations of motion derived from the Lagrangian, including damping terms. We employ periodic boundary conditions and integrate the differential equations using Heun's method with a step size $\Delta t = 2.5$ as. Here, we focus on zero temperature, where the in-plane dynamics is silent. An example of Higgs mode mediated enhancement at nonzero temperature is included in the Supplemental Material [32].

We drive the system by adding $(\omega_{\text{dr}} E_0 / \epsilon_z) \sin(\omega_{\text{dr}} t)$ to the equations of motion for the vector potential $A_{z,\mathbf{r}}(t)$ on all interlayer bonds, which describes a spatially homogeneous driving field. Note that Eqs. (1) and (2) can be derived as the Euler-Lagrange equations of the Lagrangian (7) at zero temperature. In that case, the fields are uniform in the bulk, i.e., $\psi_{\mathbf{r}} \equiv \psi$, $A_{x,\mathbf{r}} = A_{y,\mathbf{r}} \equiv 0$, and $A_{z,\mathbf{r}} \equiv A$. The equations of motion read

$$\partial_t^2 A = \frac{2ed_z t_z}{i\hbar \epsilon_z \epsilon_0} |\psi|^2 (e^{ia} - e^{-ia}) - \gamma_J \partial_t A + \frac{\omega_{\text{dr}} E_0}{\epsilon_z} \sin(\omega_{\text{dr}} t) \quad (11)$$

and

$$\partial_t^2 \psi = \frac{\mu - g|\psi|^2 + t_z(e^{ia} + e^{-ia} - 2)}{K \hbar^2} \psi - \gamma_H \partial_t \psi, \quad (12)$$

where $a = -2ed_z A/\hbar$. To recover Eqs. (1) and (2), the order parameter is expanded around its equilibrium value $\psi_0 = \sqrt{\mu/g}$, i.e., $\psi = \psi_0 + h$, and only linear terms in a and h except for the coupling term $\sim ah$ are retained. Thus, one can identify the plasma frequency with $\omega_J = \sqrt{t_z/\alpha K \hbar^2}$ and the Higgs frequency with $\omega_H = \sqrt{2\mu/K \hbar^2}$, where $\alpha = (\epsilon_z \epsilon_0)/(8K \psi_0^2 e^2 d_z^2)$ is the capacitive coupling constant of the c -axis junctions. The drive induces a current with Fourier amplitude $|j_{\text{dr}}| = ed_z \omega_{\text{dr}} E_0 / \hbar \epsilon_z$.

IV. NUMERICAL RESULTS

In the following, we present our numerical results. We evaluate the effective interlayer coupling based on the optical conductivity at $\omega_{\text{pr}} = \omega_H/120$. For weak driving, we find decent agreement between the analytical prediction in Eq. (5) and the numerical results of the full lattice gauge model, as shown in Fig. 2. The deviations are due to higher-order terms ignored in the minimal model and the perturbative expansion. They grow with increasing field strength. Nevertheless, our simulations demonstrate that the enhancement effect persists for strong driving, even in the presence of higher-order nonlinearities, fully included in our $U(1)$ lattice gauge theory.

We find that the renormalization of the interlayer coupling does not only depend on the driving parameters, but also on the ratio of the Higgs frequency and the plasma frequency of the system. Our main proposal consists of driving the superconductor slightly blue-detuned from the Higgs frequency ω_H . This mechanism is effective for all ratios of ω_J/ω_H . As we discuss below, there is a second regime in which dynamical stabilization can be achieved, if the system fulfills the requirement $\omega_H < \omega_J < \sqrt{3}\omega_H$.

Figure 3 displays the renormalized interlayer coupling as a function of the driving parameters for a monolayer cuprate with $\omega_J < \omega_H$ [the same system as in Figs. 1 and 2(a)]. Consistent with our analytical prediction, the interlayer transport is enhanced for driving frequencies blue-detuned from the Higgs frequency, while it is diminished on the red-detuned side, as immediately apparent for weak driving. In general, higher field strengths amplify the suppression/enhancement effects and additionally renormalize the Higgs frequency and the plasma frequency. The frequency renormalization of the Higgs mode results in the bending of the enhancement regime towards lower driving frequencies for larger driving fields. This observation reflects the general behavior of nonlinear oscillators to display amplitude-dependent eigenfrequencies [36]. We emphasize that the interlayer coupling can be increased by more than 50% in this example. The strongest suppression of interlayer transport occurs for driving close to the plasma frequency. This is generally the case if $\omega_J < \omega_H$ or $\omega_J > \sqrt{3}\omega_H$.

The enhancement and suppression effects are limited by heating that dominates for larger field strengths (see also Ref. [17]). We identify the heating regime based on the condition that the condensate is completely depleted. Specifically, we observe the driven dynamics for 100 ps and apply

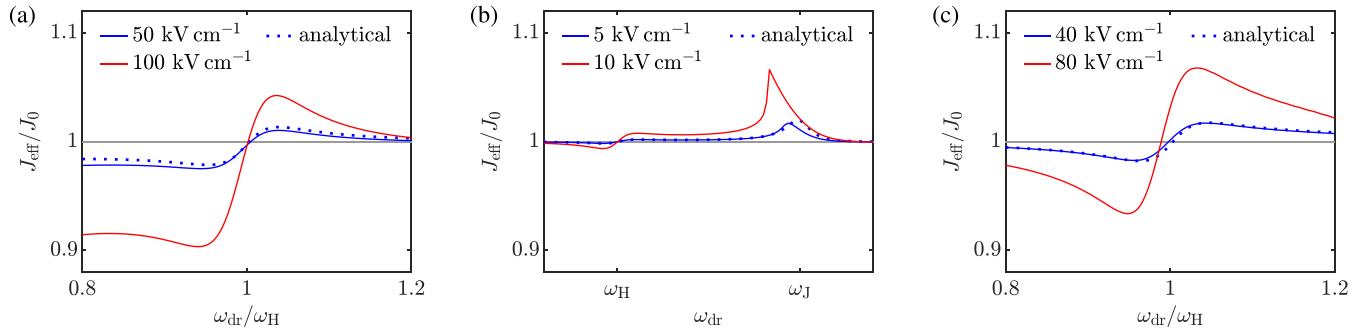


FIG. 2. Effective interlayer coupling for three light-driven monolayer cuprate superconductors with different ratios ω_J/ω_H . (a) $\omega_J < \omega_H$, (b) $\omega_H < \omega_J < \sqrt{3}\omega_H$, (c) $\sqrt{3}\omega_H < \omega_J$. Each panel shows the dependence on the driving frequency ω_{dr} for two fixed values of the field strength E_0 . Solid lines correspond to numerical results, and dotted lines indicate analytical results for the lower field strength. In all cases, the Higgs frequency is fixed at $\omega_H/2\pi = 6$ THz, while the plasma frequency $\omega_J/2\pi$ is varied: (a) 2 THz, (b) 9 THz, and (c) 15 THz.

the condition $\min(|\psi|/|\psi_0|) < 10^{-3}$ to determine unstable states. We note that the heating regime has a similar shape as the parameter set for which no stable solutions can be found by applying the harmonic balance method with ten harmonics [32,37].

Within our analytical solution for the optical conductivity in Eq. (5), we have determined an upper boundary for the driving frequency of $\sqrt{3}\omega_H$ for the enhancement effect to occur. At this boundary, the second term in the denominator of Eq. (5) switches sign. Our simulations confirm this prediction for $\omega_H < \omega_J$. However, as visible in Fig. 3, an additional suppression lowers this upper bound for superconductors with $\omega_J < (\sqrt{3} - 1)\omega_H$. Here, the enhancement regime is approximately limited by the resonance frequency of the time crystalline state at $\omega_{\text{dr}} = \omega_H + \omega_J$ [17]. This modified upper bound derives from higher-order terms not included in the analytical solution.

We continue our analysis by varying the damping coefficients, as shown in Fig. 4. Studying higher values of γ_H is particularly interesting because the damping of the Higgs mode is typically strong in cuprate superconductors [25,26]. It can be seen in Fig. 4(a) that increasing γ_H significantly decreases the enhancement of the interlayer coupling for a given field strength. By contrast, stronger damping of the

plasma mode has a negligible effect. In the Supplemental Material [32], we provide a parameter scan of the renormalized interlayer coupling with higher damping coefficients $\gamma_H/2\pi = \gamma_J/2\pi = 1$ THz. Compared to Fig. 3, we find that the parameter regime with an enhancement of more than 10% is smaller and shifted to higher field strengths.

Finally, we consider cuprates with $\omega_H < \omega_J < \sqrt{3}\omega_H$. In this case, the previous suppression of interlayer transport for $\omega_{\text{dr}} \approx \omega_J$ switches to strong enhancement, as exemplified in Fig. 2(b). Therefore, we propose to drive these particular systems near the plasma frequency ω_J . In typical monolayer cuprates, such as $\text{La}_{2-x}\text{Sr}_x\text{CuO}_4$ (LSCO), the superconducting gap 2Δ is larger than the Josephson plasma energy $\hbar\omega_J$ [38–40]. At low temperatures, the Higgs frequency approximately equals $2\Delta/\hbar$ [27,41], so it is larger than the Josephson plasma frequency in these materials, i.e., $\omega_J < \omega_H$. However, while the temperature dependence of the Higgs mode in cuprate superconductors is the subject of debate [25,26,42,43], the case $\omega_H < \omega_J < \sqrt{3}\omega_H$ might be realized for higher temperatures. For these temperatures, stronger damping and thermal fluctuations might suppress or reduce the enhancement mechanism. This regime will be discussed elsewhere. Further decay channels of the Higgs mode have been studied in Refs. [44,45].

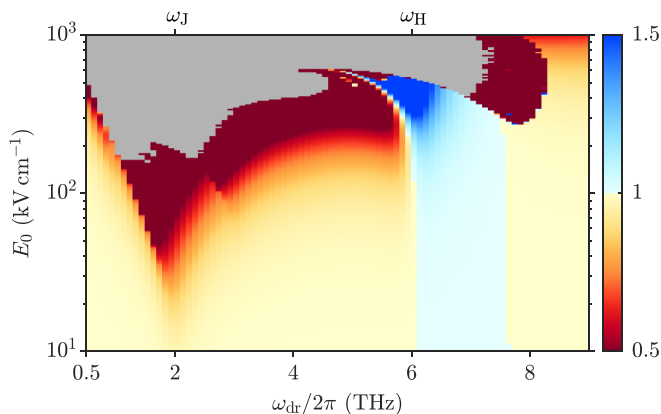


FIG. 3. Dependence of the effective interlayer coupling J_{eff}/J_0 on the driving frequency ω_{dr} and the field strength E_0 . The gray area marks the heating regime.

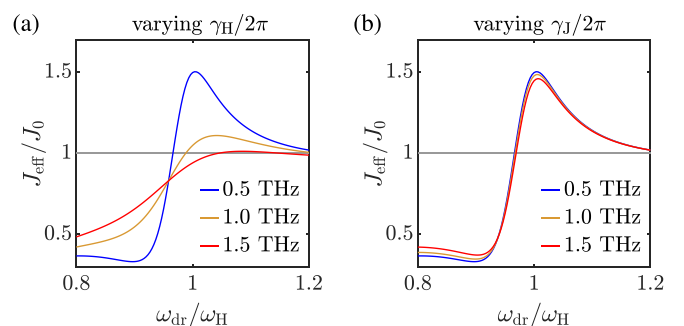


FIG. 4. Dependence of the Higgs mode mediated renormalization of the interlayer coupling on the damping coefficients. (a) γ_H is varied while $\gamma_J/2\pi = 0.5$ THz is fixed. (b) γ_J is varied while $\gamma_H/2\pi = 0.5$ THz is fixed. The cuprate with Josephson plasma frequency $\omega_J/2\pi = 2$ THz and Higgs frequency $\omega_H/2\pi = 6$ THz is driven with the field strength $E_0 = 300$ kV/cm.

V. CONCLUSION

In conclusion, we propose a mechanism for light-enhanced interlayer transport in cuprate superconductors by optically exciting Higgs oscillations which then induce a parametric amplification of the superconducting response. Both our analytical and numerical calculations show that the superconducting response of a monolayer cuprate is significantly amplified when the optical driving is slightly blue-detuned from the Higgs frequency. Our calculations demonstrate that the regime of driving parameters, for which a significant Higgs mode mediated enhancement of interlayer transport is achieved, crucially depends on the damping of the Higgs mode. Therefore, we propose to verify this effect first for low temperatures. The enhancement mechanism presented in this work is broadly applicable to cuprate superconductors because it does not rely on the existence of suitable phonons. Instead, the light-driven renormalization of interlayer transport is mediated by Higgs oscillations of the Cooper pair condensate itself. This effect amounts to dynamical control of a functionality in high-temperature superconductors, utilizing the intrinsic collective modes of these materials and their nonlinear coupling.

ACKNOWLEDGMENTS

This work is supported by the Deutsche Forschungsgemeinschaft (DFG) in the framework of SFB 925, Project No. 170620586, and the Cluster of Excellence ‘‘Advanced

TABLE I. Model parameters used in the simulations.

K (meV ⁻¹)	1.38×10^{-5}
μ (meV)	4.24×10^{-3}
g (meV Å ³)	2.12
ϵ_{xy}	1
ϵ_z	4
d_{xy} (Å)	20
d_z (Å)	10
t_{xy} (meV)	2.2×10^{-1}
t_z (meV)	$9.44 \times 10^{-4}, 1.91 \times 10^{-2}, 5.31 \times 10^{-2}$

Imaging of Matter’’ (EXC 2056), Project No. 390715994. J.O. acknowledges support by the Georg H. Endress Foundation.

APPENDIX: MODEL PARAMETERS

Table I summarizes the parameters of the monolayer cuprate superconductors studied in this paper. Our parameter choice of μ and g implies an equilibrium condensate density $n_0 = \mu/g = 2 \times 10^{21}$ cm⁻³ at zero temperature. The capacitive coupling constant is given by

$$\alpha = \frac{g\epsilon_z\epsilon_0}{8\mu K e^2 d_z^2} = 1. \quad (\text{A1})$$

For the c -axis plasma frequency, we consider the three cases $\omega_J/2\pi = 2$ THz, $\omega_J/2\pi = 9$ THz, and $\omega_J/2\pi = 15$ THz. The Higgs frequency is $\omega_H/2\pi = 6$ THz in each case.

-
- [1] D. Fausti, R. I. Tobey, N. Dean, S. Kaiser, A. Dienst, M. C. Hoffmann, S. Pyon, T. Takayama, H. Takagi, and A. Cavalleri, Light-induced superconductivity in a stripe-ordered cuprate, *Science* **331**, 189 (2011).
- [2] M. Buzzi, D. Nicoletti, M. Fechner, N. Tancogne-Dejean, M. A. Sentef, A. Georges, T. Biesner, E. Uykur, M. Dressel, A. Henderson, T. Siegrist, J. A. Schlueter, K. Miyagawa, K. Kanoda, M.-S. Nam, A. Ardavan, J. Coulthard, J. Tindall, F. Schlawin, D. Jaksch *et al.*, Photomolecular High-Temperature Superconductivity, *Phys. Rev. X* **10**, 031028 (2020).
- [3] M. Budden, T. Gebert, M. Buzzi, G. Jotzu, E. Wang, T. Matsuyama, G. Meier, Y. Laplace, D. Pontiroli, M. Riccò, F. Schlawin, D. Jaksch, and A. Cavalleri, Evidence for metastable photo-induced superconductivity in K₃C₆₀, *Nat. Phys.* **17**, 611 (2021).
- [4] W. Hu, S. Kaiser, D. Nicoletti, C. R. Hunt, I. Gierz, M. C. Hoffmann, M. Le Tacon, T. Loew, B. Keimer, and A. Cavalleri, Optically enhanced coherent transport in YBa₂Cu₃O_{6.5} by ultrafast redistribution of interlayer coupling, *Nat. Mater.* **13**, 705 (2014).
- [5] S. Kaiser, C. R. Hunt, D. Nicoletti, W. Hu, I. Gierz, H. Y. Liu, M. Le Tacon, T. Loew, D. Haug, B. Keimer, and A. Cavalleri, Optically induced coherent transport far above T_c in underdoped YBa₂Cu₃O_{6+ δ} , *Phys. Rev. B* **89**, 184516 (2014).
- [6] M. Först, A. Frano, S. Kaiser, R. Mankowsky, C. R. Hunt, J. J. Turner, G. L. Dakovski, M. P. Miniti, J. Robinson, T. Loew, M. Le Tacon, B. Keimer, J. P. Hill, A. Cavalleri, and S. S. Dhesi, Femtosecond x rays link melting of charge-density wave correlations and light-enhanced coherent transport in YBa₂Cu₃O_{6.6}, *Phys. Rev. B* **90**, 184514 (2014).
- [7] K. A. Cremin, J. Zhang, C. C. Homes, G. D. Gu, Z. Sun, M. M. Fogler, A. J. Millis, D. N. Basov, and R. D. Averitt, Photoenhanced metastable c -axis electrostatics in stripe-ordered cuprate La_{1.885}Ba_{0.115}CuO₄, *Proc. Natl. Acad. Sci. USA* **116**, 19875 (2019).
- [8] R. Mankowsky, A. Subedi, M. Först, S. O. Mariager, M. Chollet, H. T. Lemke, J. S. Robinson, J. M. Glowia, M. P. Miniti, A. Frano, M. Fechner, N. A. Spaldin, T. Loew, B. Keimer, A. Georges, and A. Cavalleri, Nonlinear lattice dynamics as a basis for enhanced superconductivity in YBa₂Cu₃O_{6.5}, *Nature (London)* **516**, 71 (2014).
- [9] S. J. Denny, S. R. Clark, Y. Laplace, A. Cavalleri, and D. Jaksch, Proposed Parametric Cooling of Bilayer Cuprate Superconductors by Terahertz Excitation, *Phys. Rev. Lett.* **114**, 137001 (2015).
- [10] R. Höppner, B. Zhu, T. Rexin, A. Cavalleri, and L. Mathey, Redistribution of phase fluctuations in a periodically driven cuprate superconductor, *Phys. Rev. B* **91**, 104507 (2015).
- [11] Z. M. Raines, V. Stanev, and V. M. Galitski, Enhancement of superconductivity via periodic modulation in a three-dimensional model of cuprates, *Phys. Rev. B* **91**, 184506 (2015).

- [12] A. A. Patel and A. Eberlein, Light-induced enhancement of superconductivity via melting of competing bond-density wave order in underdoped cuprates, *Phys. Rev. B* **93**, 195139 (2016).
- [13] J.-i. Okamoto, A. Cavalleri, and L. Mathey, Theory of Enhanced Interlayer Tunneling in Optically Driven High- T_c Superconductors, *Phys. Rev. Lett.* **117**, 227001 (2016).
- [14] J.-i. Okamoto, W. Hu, A. Cavalleri, and L. Mathey, Transiently enhanced interlayer tunneling in optically driven high- T_c superconductors, *Phys. Rev. B* **96**, 144505 (2017).
- [15] S. Rajasekaran, E. Casandruc, Y. Laplace, D. Nicoletti, G. D. Gu, S. R. Clark, D. Jaksch, and A. Cavalleri, Parametric amplification of a superconducting plasma wave, *Nat. Phys.* **12**, 1012 (2016).
- [16] F. Schlawin, A. S. D. Dietrich, M. Kiffner, A. Cavalleri, and D. Jaksch, Terahertz field control of interlayer transport modes in cuprate superconductors, *Phys. Rev. B* **96**, 064526 (2017).
- [17] G. Homann, J. G. Cosme, and L. Mathey, Higgs time crystal in a high- T_c superconductor, *Phys. Rev. Research* **2**, 043214 (2020).
- [18] T. Koyama and M. Tachiki, I - V characteristics of Josephson-coupled layered superconductors with longitudinal plasma excitations, *Phys. Rev. B* **54**, 16183 (1996).
- [19] D. van der Marel and A. A. Tsvetkov, Transverse-optical Josephson plasmons: Equations of motion, *Phys. Rev. B* **64**, 024530 (2001).
- [20] T. Koyama, Josephson plasma resonances and optical properties in high- T_c superconductors with alternating junction parameters, *J. Phys. Soc. Jpn.* **71**, 2986 (2002).
- [21] M. Harland, S. Brener, A. I. Lichtenstein, and M. I. Katsnelson, Josephson lattice model for phase fluctuations of local pairs in copper oxide superconductors, *Phys. Rev. B* **100**, 024510 (2019).
- [22] D. Dulić, A. Pimenov, D. van der Marel, D. M. Broun, S. Kamal, W. N. Hardy, A. A. Tsvetkov, I. M. Sutjaha, R. Liang, A. A. Menovsky, A. Loidl, and S. S. Saxena, Observation of the Transverse Optical Plasmon in $\text{SmLa}_{0.8}\text{Sr}_{0.2}\text{CuO}_{4-\delta}$, *Phys. Rev. Lett.* **86**, 4144 (2001).
- [23] H. Shibata and T. Yamada, Double Josephson Plasma Resonance in T^* Phase $\text{SmLa}_{1-x}\text{Sr}_x\text{CuO}_{4-\delta}$, *Phys. Rev. Lett.* **81**, 3519 (1998).
- [24] D. N. Basov and T. Timusk, Electrodynamics of high- T_c superconductors, *Rev. Mod. Phys.* **77**, 721 (2005).
- [25] K. Katsumi, N. Tsuji, Y. I. Hamada, R. Matsunaga, J. Schneeloch, R. D. Zhong, G. D. Gu, H. Aoki, Y. Gallais, and R. Shimano, Higgs Mode in the d -Wave Superconductor $\text{Bi}_2\text{Sr}_2\text{CaCu}_2\text{O}_{8+x}$ Driven by an Intense Terahertz Pulse, *Phys. Rev. Lett.* **120**, 117001 (2018).
- [26] H. Chu, M.-J. Kim, K. Katsumi, S. Kovalev, R. D. Dawson, L. Schwarz, N. Yoshikawa, G. Kim, D. Putzky, Z. Z. Li, H. Raffy, S. Germanskiy, J.-C. Deinert, N. Awari, I. Ilyakov, B. Green, M. Chen, M. Bawatna, G. Christiani, G. Logvenov *et al.*, Phase-resolved Higgs response in superconducting cuprates, *Nat. Commun.* **11**, 1793 (2020).
- [27] R. Shimano and N. Tsuji, Higgs mode in superconductors, *Annu. Rev. Condens. Matter Phys.* **11**, 103 (2020).
- [28] C. M. Varma, Higgs boson in superconductors, *J. Low Temp. Phys.* **126**, 901 (2002).
- [29] D. Pekker and C. Varma, Amplitude/Higgs modes in condensed matter physics, *Annu. Rev. Condens. Matter Phys.* **6**, 269 (2015).
- [30] Z. Sun, M. M. Fogler, D. N. Basov, and A. J. Millis, Collective modes and terahertz near-field response of superconductors, *Phys. Rev. Research* **2**, 023413 (2020).
- [31] M. Machida and T. Koyama, Localized rotating-modes in capacitively coupled intrinsic Josephson junctions: Systematic study of branching structure and collective dynamical instability, *Phys. Rev. B* **70**, 024523 (2004).
- [32] See Supplemental Material at <http://link.aps.org/supplemental/10.1103/PhysRevB.103.224503> for a detailed derivation of the analytical prediction in Eq. (5), details of the lattice gauge model, a comparison between the quadratic and fully nonlinear models, a discussion of the condensate depletion, results for different values of the damping coefficients and the capacitive coupling constant, and finite-temperature results.
- [33] V. L. Ginzburg and L. D. Landau, On the theory of superconductivity, *Zh. Eksp. Teor. Fiz.* **20**, 1064 (1950).
- [34] J. B. Kogut, An introduction to lattice gauge theory and spin systems, *Rev. Mod. Phys.* **51**, 659 (1979).
- [35] K. Yee, Numerical solution of initial boundary value problems involving Maxwell's equations in isotropic media, *IEEE Trans. Antennas Propag.* **14**, 302 (1966).
- [36] L. D. Landau and E. M. Lifshitz, *Mechanics*, 3rd ed. (Butterworth-Heinemann, Oxford, U.K., 1976).
- [37] J. C. Slater, Mousai: An open-source general purpose harmonic balance solver, 13th ASME Dayton Engineering Sciences Symposium, 2017, <https://josephslater.github.io/DESS2017/>.
- [38] S. V. Dordevic, S. Komiya, Y. Ando, and D. N. Basov, Josephson Plasmon and Inhomogeneous Superconducting State in $\text{La}_{2-x}\text{Sr}_x\text{CuO}_4$, *Phys. Rev. Lett.* **91**, 167401 (2003).
- [39] G. Deutscher, Coherence and single-particle excitations in the high-temperature superconductors, *Nature (London)* **397**, 410 (1999).
- [40] M. Hashimoto, T. Yoshida, K. Tanaka, A. Fujimori, M. Okusawa, S. Wakimoto, K. Yamada, T. Kakeshita, H. Eisaki, and S. Uchida, Distinct doping dependences of the pseudogap and superconducting gap of $\text{La}_{2-x}\text{Sr}_x\text{CuO}_4$ cuprate superconductors, *Phys. Rev. B* **75**, 140503(R) (2007).
- [41] F. Yang and M. W. Wu, Theory of Higgs modes in d -wave superconductors, *Phys. Rev. B* **102**, 014511 (2020).
- [42] M. Puviani, A. Baum, S. Ono, Y. Ando, R. Hackl, and D. Manske, Enhanced A_{1g} Raman response in cuprates due to Higgs oscillations, [arXiv:2012.01922](https://arxiv.org/abs/2012.01922).
- [43] F. Gabriele, M. Udina, and L. Benfatto, Non-linear terahertz driving of plasma waves in layered cuprates, *Nat. Commun.* **12**, 752 (2021).
- [44] F. Peronaci, M. Schiró, and M. Capone, Transient Dynamics of d -Wave Superconductors After a Sudden Excitation, *Phys. Rev. Lett.* **115**, 257001 (2015).
- [45] Y. Murakami, P. Werner, N. Tsuji, and H. Aoki, Damping of the collective amplitude mode in superconductors with strong electron-phonon coupling, *Phys. Rev. B* **94**, 115126 (2016).